Available online at www.sciencedirect.com

ScienceDirect

Chinese Journal of Natural Medicines 2021, **19**(4): 305-320
doi: 10.1016/S1875-5364(21)60031-6

Chinese Journal of Natural Medicines

•Research article•

Comprehensive profiling and characterization of the absorbed components and metabolites in mice serum and tissues following oral administration of Qing-Fei-Pai-Du decoction by UHPLC-Q-Exactive-Orbitrap HRMS

LIU Wei[1Δ], HUANG Jian[2Δ], ZHANG Feng[2], ZHANG Cong-Cong[1, 3], LI Rong-Sheng[1], WANG Yong-Li[3], WANG Chao-Ran[4], LIANG Xin-Miao[4], ZHANG Wei-Dong[2], YANG Ling[2], LIU Ping[1, 2*], GE Guang-Bo[2*]

[1] *Key Laboratory of Liver and Kidney Diseases (Ministry of Education), Institute of Liver Diseases, Shanghai Key Laboratory of Traditional Chinese Clinical Medicine, Shuguang Hospital Affiliated to Shanghai University of Traditional Chinese Medicine, Shanghai 201203, China;*

[2] *Institute of Interdisciplinary Integrative Medicine Research, Shanghai University of Traditional Chinese Medicine, Shanghai 201203, China;*

[3] *Institute of Chinese Materia Medica, Shanghai University of Traditional Chinese Medicine, Shanghai 201203, China;*

[4] *Dalian Institute of Chemical Physics, Chinese Academy of Sciences, Dalian 116023, China*

Available online 20 Apr., 2021

[ABSTRACT] Qing-Fei-Pai-Du decoction (QFPDD) is a Chinese medicine compound formula recommended for combating corona virus disease 2019 (COVID-19) by National Health Commission of the People's Republic of China. The latest clinical study showed that early treatment with QFPDD was associated with favorable outcomes for patient recovery, viral shedding, hospital stay, and course of the disease. However, the effective constituents of QFPDD remain unclear. In this study, an UHPLC-Q-Orbitrap HRMS based method was developed to identify the chemical constituents in QFPDD and the absorbed prototypes as well as the metabolites in mice serum and tissues following oral administration of QFPDD. A total of 405 chemicals, including 40 kinds of alkaloids, 162 kinds of flavonoids, 44 kinds of organic acids, 71 kinds of triterpene saponins and 88 kinds of other compounds in the water extract of QFPDD were tentatively identified *via* comparison with the retention times and MS/MS spectra of the standards or refereed by literature. With the help of the standards and *in vitro* metabolites, 195 chemical components (including 104 prototypes and 91 metabolites) were identified in mice serum after oral administration of QFPDD. In addition, 165, 177, 112, 120, 44, 53 constituents were identified in the lung, liver, heart, kidney, brain, and spleen of QFPDD-treated mice, respectively. These findings provided key information and guidance for further investigation on the pharmacologically active substances and clinical applications of QFPDD.

[KEY WORDS] Qing-Fei-Pai-Du decoction (QFPDD); Corona virus disease 2019 (COVID-19); Chemical profiling; Absorbed components; High-Resolution Mass Spectrometry (HRMS)

[CLC Number] R917 **[Document code]** A **[Article ID]** 2095-6975(2021)04-0305-16

[Received on] 06-Feb.-2021

[Research funding] This work was supported by the National Key Research and Development Program of China (2020YFC0845400), the NSF of China (81922070), Shanghai Science and Technology Innovation Action Plans (20S21901500; 20S21900900) supported by Shanghai Science and Technology Committee, the Three-year Action Plan of Shanghai TCM Development (ZY-(2018-2020)-CCCX-5001), and Program of Shanghai Academic/Technology Research Leader (18XD1403600).

[*Corresponding author] E-mail: liuliver@vip.sina.com (LIU Ping); geguangbo@dicp.ac.cn (GE Guang-Bo)

[Δ]These authors contributed equally to this work.

These authors have no conflict of interest to declare.

Introduction

Corona Virus Disease 2019 (COVID-19), a newly emerged infective disease, has spread all over the world, with a long incubation period, high infectivity and general susceptibility to all types of people [1-3]. The COVID-19 global pandemic has brought significantly negative effects for human health, economic and social stability. Researchers are now trying to find effective medications (including western therapeutics and herbal medicines) for combating COVID-19, while some therapeutics and herbal medicines have been used

for treating COVID-19 in clinical settings [4-7]. In China, several Chinese medicine compound formulas, such as Qing-Fei-Pai-Du decoction (QFPDD), Jingyin granules and Lianhua Qingwen capsule, have been validated playing an active role in combating this epidemic, especially alleviating the symptoms of some moderate and mild patients [8]. Among all recommend Chinese medicines for combating COVID-19 in China, QFPDD has drawn much attention owing to its effectiveness of COVID-19. As the first Chinese medicine compound formula recommended by National Health Commission of the People's Republic of China for combating COVID-19, QFPDD has been used to treat thousands of COVID-19 patients with the total effective rate of 97% [9-12]. Following oral administration of QFPDD, the major symptoms and imaging manifestations of more than 60% patients were significantly improved, while the symptoms of 30% patients were stable and did not aggravate [13]. Early treatment with QFPDD is associated with favorable outcomes for patient recovery, viral shedding, hospital stay, and course of the disease. And early treatment with QFPDD may serve as an effective strategy in controlling the epidemic [14].

Unlike Western therapeutics, Chinese medicines are always the mixtures of a wide range of ingredients, these ingredients as well as their *in vivo* metabolites may interact with a wide range of targets in the human body in an extremely complex way [15, 16]. To better understand the material basis for efficacy of QFPDD, the chemical constituents in this anti-COVID-19 Chinese medicine and the key components (including prototypes and metabolites) occurring in serum and target organs (such as the lung and the liver) following QFPDD treatment should be carefully investigated. Notably, QFPDD is deriving from four classic Chinese medicine prescriptions (including Maxing Shigan decoction, Shegan Mahuang decoction, Xiaochaihu decoction, and Wuling powder) that are used for treating epidemic diseases and the related inflammatory symptoms for thousands of years [17-20]. As a super combination of 20 herbs and a mineral drug (*Gypsum Fibrosum*), QFPDD is composed by hundreds of ingredients and parts of them may be absorbed in circulation system and then exert their bioactivites, such as anti-inflammatory and anticoagulation effects [21, 22]. However, the chemical constituents in QFPDD and the absorbed components of this Chinese medicine have not been well-investigated yet, which strongly block further investigations on the pharmacological and toxicological studies, the quality control and clinical applications of this anti-COVID-19 Chinese medicine.

This study aims to investigate the main chemical constituents in QFPDD and the absorbed components (including prototypes and metabolites) in serum and tissues after oral administration of QFPDD to mice. To this end, an UHPLC-Q-Orbitrap HRMS based method was well-established for systematic profiling the constituents in QFPDD, while the absorbed components (including the prototypes and the metabolites) occurring in mouse serum and tissues were also identified *via* profiling the serum and tissue samples from QFPDD-treated mice. The prototype components in both QFPDD and mouse serum were tentatively identified *via* comparison with the retention times and MS/MS spectra of the standards or refereed by literature, while the *in vivo* metabolites were tentatively identified *via* comparison with the retention times and MS/MS spectra of the *in vitro* metabolites generated in mice liver microsomes (MLMs). Finally, a total of 405 chemicals (including 40 kinds of alkaloids, 162 kinds of flavonoids, 44 kinds of organic acids, 71 kinds of triterpene saponins and 88 kinds of other compounds) in the water extract of QFPDD were identified, while 195, 165, 177, 112, 120, 44, 53 constituents were identified in the serum, lung, liver, heart, kidney, brain, and spleen of QFPDD-treated mice, respectively. All these findings are very helpful for deep understanding the fates of the constituents in QFPDD, as well as the key information of the tissue distribution of the absorbed components of this anti-COVID-19 Chinese medicine.

Materials and Methods

Chemicals and materials

Herba Ephedrae (Mahuang, No. 191119-1), *Ramulus Cinnamoni* (Guizhi, No. 190802-1), *Rhizoma Alismatis* (Zixie, No. 191031-1), *Polyporus* (Zhuling, No. 191109-1), *Flos Farfarae* (Kuandonghua, No. 191207-1), Herba Asari (Xixin, No. 191220-1) and *Rhizoma Dioscoreae* (Shanyao, No. 191023-1) were purchased from Shanghai Wanshicheng Pharmaceutical Co., Ltd. (Shanghai, China). *Gypsum Fibrosum* (Shengshigao, No. 190801), *Poria* (Fuling, No. 191218), *Radix Bupleuri* (Chaihu, No. 200103), *Rhizoma Pinelliae* prepared with ginger juice (Jiangbanxia, No. 191009) and *Herba Agastachis* (Huoxiang, No. 190814) were purchased from Shanghai Hongqiao Traditional Chinese Medicine Decoction Piecess Co., Ltd. (Shanghai, China). *Radix Glycyrrhizae Praeparata* (Zhigancao, No. 191213), *Rhizoma Belamcandae* (Shegan, No. 191022), *Fructus Aurantii Immaturus* (Zhishi, No. 200119), *Semen Armeniaceae Amarum* (Xingren, No. 200108) were purchased from Shanghai Kangqiao Traditional Chinese Medicine Decoction Piecess Co., Ltd. (Shanghai, China). *Radix Scutellariae* (Huangqin, No. 19112307), *Radix Asteris* (Ziwan, No. 1909247) and *Pericarpium Citri Reticulatae* (Chenpi, No. 191119) were purchased from Shanghai Yanghetang Traditional Chinese Medicine Decoction Piecess Co., Ltd. (Shanghai, China). *Rhizoma Atractylodis Macrocephalae* (Baizhu, No. 190830) was purchased from Shanghai Qingpu Traditional Chinese Medicine Decoction Piecess Co., Ltd. (Shanghai, China). Fresh *Rhizoma Zingiberis Recens* (Shengjiang) was purchased from the supermarket. All of the herbs were authenticated by prof. WANG Chang-Hong, from the Institute of Chinese Materia Medica, Shanghai University of Traditional Chinese Medicine.

Arginine, uridine, uracil, tyrosine, leucine, isoleucine, adenine, 6-hydroxypurine, guanine, guanosine, adenosine, xanthosine, L-phenylalanine, tryptophan were purchased from Dalian Meilun Biotechnology Co. Ltd. (Dalian, China). Neochlorogenic acid, caffeic acid, chlorogenic acid, crypto-

chlorogenic acid, L-amygdalin, prunasin, 1,3-*O*-dicaffeoylquinic acid, ferulic acid, isochlorogenic acid B, isochlorogenic acid A, resveratrol, isochlorogenic acid C, tilianin, 6-Gingerol, 8-gingerol, 10-gingerol, alisol B-23-acetate and pachymic acid were purchased from Chengdu Biopurify Phytochemicals Ltd. (Chengdu, China). Quinic acid, stachydrine, citric acid, succinic acid, gallic acid, synephrine, phenylpropanolamine, D-demethyl pseudoephedrine, vanillic acid, ephedrine, pseudoephedrine, methylephedrine, catechin, epicatechin, neoliquiritin, 3, 4-dihydroxybenzaldehyde, luteolin-7-*O*-*β*-D-glucoside, liquiritin, vitexin, tectoridin, isovitexin, hyperin, scutellarin, quercetin, isoquercitrin, verbascoside, hesperetin, isoaceteoside, hesperidin, astragalin, neohesperidin, cinnamaldehyde, liquiritigenin, isoliquiritin, ononin, naringin, luteolin, baicalin, cinnamic acid, naringenin, licochalcone A, licochalcone B, wogonoside, kaempferol, rosmarinic acid, isoliquiritigenin, baicalein, formononetin, sinensetin, irisflorentin, oroxylin A, nobiletin, atractylenolide-I, tangeretin, asarinin, glycyrrhizic acid, tussilagone and alisol A were provided by Prof. LIANG Xin-Miao from Dalian Institute of Chemical Physics, Chinese Academy of Sciences (Dalian, China). The purities of those reference substances were more than 98%.

Glucose 6-phosphate (G-6-P), glucose-6-phosphate dehydrogenase (G-6-PDH), nicotinamide adenine dinucleotide phosphate disodium salt (*β*-$NADP^+$), uridine di-phosphate glucuronic acid (UDPGA), alamethicin, *S*-adenosyl-L-methionine (SAM) and 3-phosphoadenosine 5-phosphosulfate (PAPS) were purchased from Sigma Aldrich Co. (St. Louis, MO, USA). Tris base and $MgCl_2$ were purchased from Majorbio Biotech Corp., Ltd. (Shanghai, China). Pooled liver microsomes from male ICR/CD-1 mouse (MLM, Lot no. STOM) was ordered from Research Institute for Liver Diseases (RILD, Shanghai, China). Acetonitrile, methanol and formic acid of HPLC grade were purchased from Fisher Scientific Co. (Santa Clara, USA). Deionized water was produced with a Milli-Q Academic System (Millipore, Billerica, MA). All other reagents and solvents were either analytical or HPLC grade.

Preparation of the Chinese multi-herbal formula QFPDD

The Chinese multi-herbal formula Qing-Fei-Pai-Du decoction (QFPDD) was prepared according to the following procedure, pieces of Herba Ephedrae (Mahuang) 45 g, Radix Glycyrrhizae Praeparata (Zhigancao) 30 g, Semen Armeniaceae Amarum (Xingren) 45 g, Gypsum Fibrosum (Shengshigao) 75 g (fried first), Ramulus Cinnamoni (Guizhi) 45 g, Rhizoma Alismatis (Zixie) 45 g, Polyporus (Zhuling) 45 g, Rhizoma Atractylodis Macrocephalae (Baizhu) 45 g, Poria (Fuling) 75 g, Radix Bupleuri (Chaihu) 80 g, Radix Scutellariae (Huangqin) 30 g, Rhizoma Pinelliae prepared with ginger juice (Jiangbanxia) 45 g, Rhizoma Zingiberis Recens (Shengjiang) 45 g, Radix Asteris (Ziwan) 45 g, Flos Farfarae (Kuandonghua) 45 g, Rhizoma Belamcandae (Shegan) 45 g, Herba Asari (Xixin) 30 g, Rhizoma Dioscoreae (Shanyao) 60 g, Fructus Aurantii Immaturus (Zhishi) 30 g, Pericarpium Citri Reticulatae (Chenpi) 30 g and Herba Agastachis (Huoxiang) 45 g, were mixed together and macerated in 12 L deionized water for 40 min before being decocted. After then, 980 g of the herbal mixture was decocted for 45 min. A total of 100 batches of QFPDD were decocted repeatly and then combined. After filtration, the decoction (about 180 L) was further concentrated to 20 L by rotary evaporation at 40−50 °C in vacuum with a 93.98% concentrated yield. Finally, 6.52 kg powder was obtained by spray-drying with a 78.55% spray-dried yield.

Preparation of QFPDD extract

QFPDD (1.0 g) was weighed and dissolved in 125 mL deionized water by ultrasonic (250 W, 50 HZ) for 1 h. Then, the sample solution was centrifuged at 10 000 × *g* for 15 min. The supernatant solution was filtered through a 0.22 μm membrane for further analysis.

Animal handling and sampling

Twelve male C57BL/6J mice (SPF grade, weight of 20 ± 2 g) were purchased from Shanghai Slac Laboratory Animal Co. Ltd. (Shanghai, China) and were fed in Experimental Animal Center of Shanghai University of Traditional Chinese Medicine. All of animals were housed in an environment-controlled breeding room at 25 °C with a 12 hours dark/light cycle. All experiments performed in mice were in accordance with the State Committee of Science and Technology of P.R. of China, and the protocol for this study was approved and monitored by the Animal Ethics Committee of Shanghai University of Traditional Chinese Medicine (PZSHUTCM-200717018).

After seven days of acclimatization, twelve male mice were randomly divided into two groups (6 mice for each group). QFPDD group was oral administered QFPDD (18 g dried material/kg); control group was oral administered deionized water. All animals were fasted overnight before the experiments and had free access to water. One hour after the once oral administration, all mice were anesthetized, blood samples were collected from the abdominal aorta, and their various tissues (lung, liver, heart, kidney, brain, spleen) were removed rapidly. Blood samples were placed at room temperature for 1 h until solidifcation. Then, serum samples were obtained by centrifuged at 5000 $r \cdot min^{-1}$ for 15 min at 4 °C. All samples were stored at −80 °C until analysis. The serum samples (200 μL) were added five times methanol (1 mL), vortexed and then, centrifuged at 10 000 × *g* for 15 min. The supernatant (960 μL) was dried with nitrogen gas. The residue was redissolved in 80 μL 10% methanol, vortexed and then, centrifuged at 10 000 × *g* for 15 min, and the filtrate was used as the LC/MS sample. The 100 mg various tissues (lung, liver, heart, kidney, brain, spleen) were homogenized in 1 mL methanol on ice, the homogenate of them was centrifuged at 4 °C at 10 000 × *g* for 15 min, The supernatant (800 μL) was dried with nitrogen gas. The residue was redissolved in 80 μL 10% methanol, vortexed and then, centrifuged at 10 000 × *g* for 15 min, and the filtrate was used as the LC/MS sample. The supernatant (2 μL) was used in the

UHPLC-Q-Exactive Orbitrap HRMS analysis.

In vitro metabolism of the major constituents isolated from QFPDD in MLMs

Microsomal incubation with NADPH: The incubation was performed in a 50 mmol·L^{-1} Tris–HCl buffer (pH 7.4) containing MLMs (1.0 mg protein/mL), the NADPH-generating system contained 10 mmol·L^{-1} G-6-P, 1 mmol·L^{-1} $NADP^+$, 4 mmol·L^{-1} $MgCl_2$, and 1 unit·mL^{-1} G-6-PDH, and 200 μmol·L^{-1} analyte (nobiletin) which was previously dissolved in methanol with concentration 200 μmol·L^{-1} in a total volume of 200 μL with concentration 200 μmol·L^{-1} in a total volume of 200 μL [23, 24]. The final concentration of methanol in the incubation system was less than 1% (*V*/*V*). The reactions were terminated with 600 μL ice-cold acetonitrile after 60 min incubation. The mixture was centrifuged at 10 000 × *g* for 15 min, and then the supernatant (720 μL) was evaporated to dryness by a gentle stream of nitrogen (37 °C). The residue was dissolved by 90 μL of 5% methanol and centrifuged at 10 000 × *g* for 10 min. 2 μL of the supernatant was injected for UHPLC-Q-Exactive Orbitrap HRMS system. Control samples containing no NADPH or substrates were prepared. Incubation was performed in duplicate.

Microsomal incubation with NADPH and UDPGA: 200 μmol·L^{-1} analyte (baicalein, scutellarin, wogonin, norwogonin, formononetin, liquiritigenin, hesperetin, naringenin, quercetin, oroxylin A and caffeic acid, each compound was incubated separately) was mixed with alamethicin (25 μg/mg protein) and the microsomes (1.0 mg protein/mL) in 100 mmol·L^{-1} Tris-HCl buffer (50 mmol·L^{-1}, pH 7.4). After 5 min of pre-incubation at 37 °C, the incubation reaction was initiated by the addition of G-6-P (10 mmol·L^{-1}), G-6-PDH (1 unit·mL^{-1}), $NADP^+$ (1.0 mmol·L^{-1}), and UDPGA (5.0 mmol·L^{-1}). The total incubation volume was 200 μL. The final concentration of methanol in the incubation system was less than 1% (*V*/*V*). The reactions were terminated with 600 μL ice-cold acetonitrile after 1 h of incubation. The mixture was centrifuged at 10 000 × *g* for 15 min, and then the supernatant (720 μL) was evaporated to dryness by a gentle stream of nitrogen at 37 °C. The residue was dissolved by 90 μL of 5% methanol and centrifuged at 10 000 × *g* for 15 min. The supernatant (2 μL) was then injected for UHPLC-Q-Exactive Orbitrap HRMS system. Control samples without NADPH and UDPGA or substrates were prepared. Incubation was performed in duplicate.

Microsomal incubation with NADPH and PAPS: The incubation was performed in a 50 mmol·L^{-1} Tris–HCl buffer at pH 7.4 containing microsomes (1.0 mg protein/mL), the NADPH-generating system contained 10 mmol·L^{-1} G-6-P, 1 mmol·L^{-1} $NADP^+$, 4 mmol·L^{-1} $MgCl_2$, and 1 unit·mL^{-1} of G-6-PDH, 100 μmol·L^{-1} PAPS, and 200 μmol·L^{-1} analyte (baicalein, wogonin, formononetin, liquiritigenin, hesperetin and caffeic acid, each compound was incubated separately) in a total volume of 200 μL. The final concentration of methanol in the incubation system was less than 1% (*V*/*V*). The reactions were terminated with 600 μL ice-cold acetonitrile after 60 min incubation. The next process was as same as above and the control samples containing no NADPH, no PAPS or substrates were prepared. Each of the incubations was performed in duplicate.

Microsoma incubation with NADPH and SAM: The incubation was performed in a 50 mmol·L^{-1} Tris–HCl buffer at pH 7.4 containing microsomes (1.0 mg protein/mL), the NADPH-generating system contained 10 mmol·L^{-1} G-6-P, 1 mmol·L^{-1} $NADP^+$, 4 mmol·L^{-1} $MgCl_2$, and 1 unit·mL^{-1} of G-6-PDH, 100 μmol·L^{-1} SAM, and 200 μmol·L^{-1} analyte (baicalein, scutellarin, chlorogenic acid and caffeic acid, each compound was incubated separately) in a total volume of 200 μL. The final concentration of methanol in the incubation system was less than 1% (*V*/*V*). The reactions were terminated with 600 μL ice-cold acetonitrile after 60 min incubation. The next process was as same as above and the control samples containing no NADPH, no SAM or substrates were prepared. Each of the incubations was performed in duplicate.

Chromatography conditions for UHPLC-Q-Exactive Orbitrap HRMS

Chromatographic separation was performed on a UHPLC-Q-Exactive Orbitrap system (Thermo Fisher Scientific Inc., Grand Island, NY, USA). The UHPLC system consisted of a Thermo Scientific Dionex Ultimate 3000 Series RS pump coupled with a Thermo Scientific Dionex Ultimate 3000 Series TCC-3000RS column compartments and WPS-3000 autosampler controlled by Chromeleon 7.2 Software. The cooling autosampler was set at 4 °C and protected from light, and the column heater was set at 40 °C. A Waters ACQUITY UPLC BEH C_{18} column (2.1 mm × 100 mm, 1.7 μm) was employed with the temperature set at 40 °C. The mobile phase consisted of A (methanol) and B (0.1% formic acid) at a flow rate of 0.3 mL·min^{-1} and eluted with gradient elution: 0−4 min (4% A), 4−10 min (4%−12% A), 10−30 min (12%−70% A), 30−35 min (70% A), 35−38 min (70%−95% A), 38−42 min (95% A), 42−45 min (4% A). The injection volume was 2 μL.

The mass spectrometer Q-Exactive Orbitrap system was connected to the UHPLC system *via* heated electrospray ionization and controlled by Xcalibur 4.1 software that was used for data collection and analysis. The electrospray ionization source was operated and optimized in negative and positive ionization mode. The optimized parameters of mass spectrometry were: capillary temperature: 325 °C; sheath gas (N_2) flow rate: 45 arbitrary units; auxiliary gas (N_2) flow rate: 8 arbitrary units; sweep gas flow rate: 0 arbitrary units; spray voltage: 2.5 kV (negative), 3.5 kV (positive); S-lens RF level: 50V; auxilliary gas heater temperature, 300 °C; scan mode: Full MS/SIM and Full MS/dd-MS2 mode, which includes 1 first-level full scan (resolution 70000 FWHM) and 1 data-dependent secondary scan (resolution 17500 FWHM) 2 events, the scanning range is 80−1200 *m*/*z*, and the collision energy gradient is 20, 50, 100V.

Establishment of QFPDD chemical database and chemical profiling

By searching databases, such as PubMed of the US Na-

tional Library Medicine and the National Institutes of Health, SciFinder Scholar of American Chemical Society and the Chinese National Knowledge Infrastructure (CNKI) of Tsinghua University, the Encyclopedia of Traditional Chinese Medicine Database (ETCM, http://www.tcmip.cn/ETCM/index.php/Home/Index/index.html), Traditional Chinese Medicine Integrated Database (TCMID, http://www.megabionet.org/tcmid/), and all components reported in the literature on 21 herbs of QFPDD were summarized in a TraceFinder software (version 3.3) to establish a database, which includes the name, molecular formula, chemical structure and literature of each published known compound. After the sample was injected, the quasi-molecular ion information was obtained, and the molecular formula was fitted by Xcalibar 3.0 software, and matched with the CD (Compound discovery, 2.1) compound analysis and identification software and self-built database, and the possible chemical composition was inferred. Combined with the relative retention time and fragment ion information of reference substances and literature, the chemical composition was identified.

Results

Identification and characterization of chemical constituents from QFPDD

Under the optimal conditions described above, the constituents in the crude extract of QFPDD were comprehensively analyzed by UHPLC-Q-Exactive Orbitrap HRMS, with a running time of 45 min. The total ion chromatograms (TICs) of the extract of QFPDD under both positive and negative ion modes are shown in Fig. 1. The protonated molecular weights of all identified compounds were calculated within an error of 10 ppm. Following carefully comparison with the retention times and MS/MS spectra of the reference standards, reference literature, Chemical Book and self-bulit databases, a total of 405 chemicals were identified or tentatively characterized from QFPDD, including 40 kinds of alkaloids, 162 kinds of flavonoids, 44 kinds of organic acids, 71 kinds of triterpene saponins and 88 kinds of other compounds (Supplementary Table S1). The detailed information of the identified chemical constituents in QFPDD including retention time, precise molecular weight, MS/MS fragment ions and the source of each constituent, have been listed in Supplementary Table S1. Among all identified chemical constituents, ninety-one constituents are confirmed by the authentic standards.

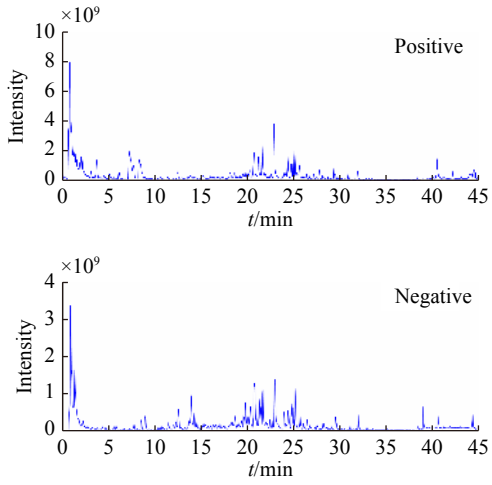

Fig. 1 The total ion chromatograms (TICs) of the extract of Qing-Fei-Pai-Du decoction by UHPLC-Q-Exactive Orbitrap HRMS

It is well-accepted that deep understanding of the fragmentation pattern of each authentic standard or its analgous is very helpful for the identification of herbal constituents by using HRMS [17]. In this study, the fragmentation pathways of various constituents (ephedrine, amygdalin, nobiletin, liquiritin, gallic acid, chlorogenic acid, saikosaponin A and glycyrrhizic acid) in QFPDD were carefully studied and proposed in Fig. 2 and Fig. 3. For example, ephedrine (t_R = 7.30 min), an abundant alkaloid distributed in *Herba Ephedrae*, could be easily detected in the positive ion mode with a quasi-molecular ion $[M + H]^+$ at *m/z* 166.1226 ($C_{16}H_{16}NO$). MS/MS fragmentation analysis demonstrated that this natural compound possessed a neutral loss of H_2O, subsequently by the cleavage of C-N bond moiety (Fig. 2A), evidenced by the product ions of *m/z* 148.1119 $[M + H - H_2O]^+$, *m/z* 133.0886 $[M + H - H_2O - CH_3]^+$, *m/z* 117.0701 $[M + H - H_2O - CH_5N]^+$ and *m/z* 91.0548 $[M + H - H_2O - CH_5N - C_2H_2]^+$. The compound **56** ($t_R$ = 7.30 min) in Supplementary Table S1 were detected in the positive ion mode at the same retention time with the identical *m/z* of 166.1225 ($C_{16}H_{16}NO$), thus was characterized as ephedrine. amygdalin (t_R = 13.93 min), an abundant alkaloid distributed in *Semen Armeniaceae Amarum*, could be easily detected in the negative ion mode with a quasi-molecular ion $[M + HCOOH - H]^-$ at *m/z* 502.1567 ($C_{21}H_{28}NO_{13}$). It was inclined to lose the whole sugar moiety to generate base peak ions *m/z* of 323.0972 $[M + HCOOH - H - C_6H_{11}O_6]^-$ and 179.0550 $[C_6H_{11}O_6]^-$ in MS^2 spectra (Fig. 2B). Subsequently by cleavage of the functional group on the second glucose, such as *m/z* of 263.0772 $[M + HCOOH - H - C_6H_{11}O_6 - C_2H_4O_2]^-$ and 221.0661 $[M + HCOOH - H - C_6H_{11}O_6 - C_7H_4N]^-$. Simultaneously the fragmentation signal of glucose was detected, its MS/MS data were shown as *m/z* of 161.0444 $[C_6H_{11}O_6 - H_2O]^-$,119.0335$[C_6H_{11}O_6–H_2O–C_2H_2O]^-$,101.0229$[C_6H_{11}O_6–H_2O - C_2H_2O - H_2O]^-$ and 89.0229 $[C_6H_{11}O_6 - H_2O - C_2H_2O - CH_2O]^-$. The compound **90** in Supplementary Table S1 were detected in the negative ion mode at 13.93 min with the identical *m/z* of 502.1568 ($C_{21}H_{28}NO_{13}$), thus this peak was characterized as amygdalin. Similar to the identification process above, a total of 40 alkaloids were identified fromdoephedrine, methylephedrine, ligustrazine, prunasin, *et al*. methylephedrine, ligustrazine, prunasin, *et al*.

Nobiletin (t_R = 29.30 min), a flavonoid distributed in Fructus Aurantii Immaturus and Pericarpium Citri Reticulatae, could be easily detected in the positive ion mode with a quasi-molecular ion $[M + H]^+$ at *m/z* 403.1385 ($C_{21}H_{23}O_8$).

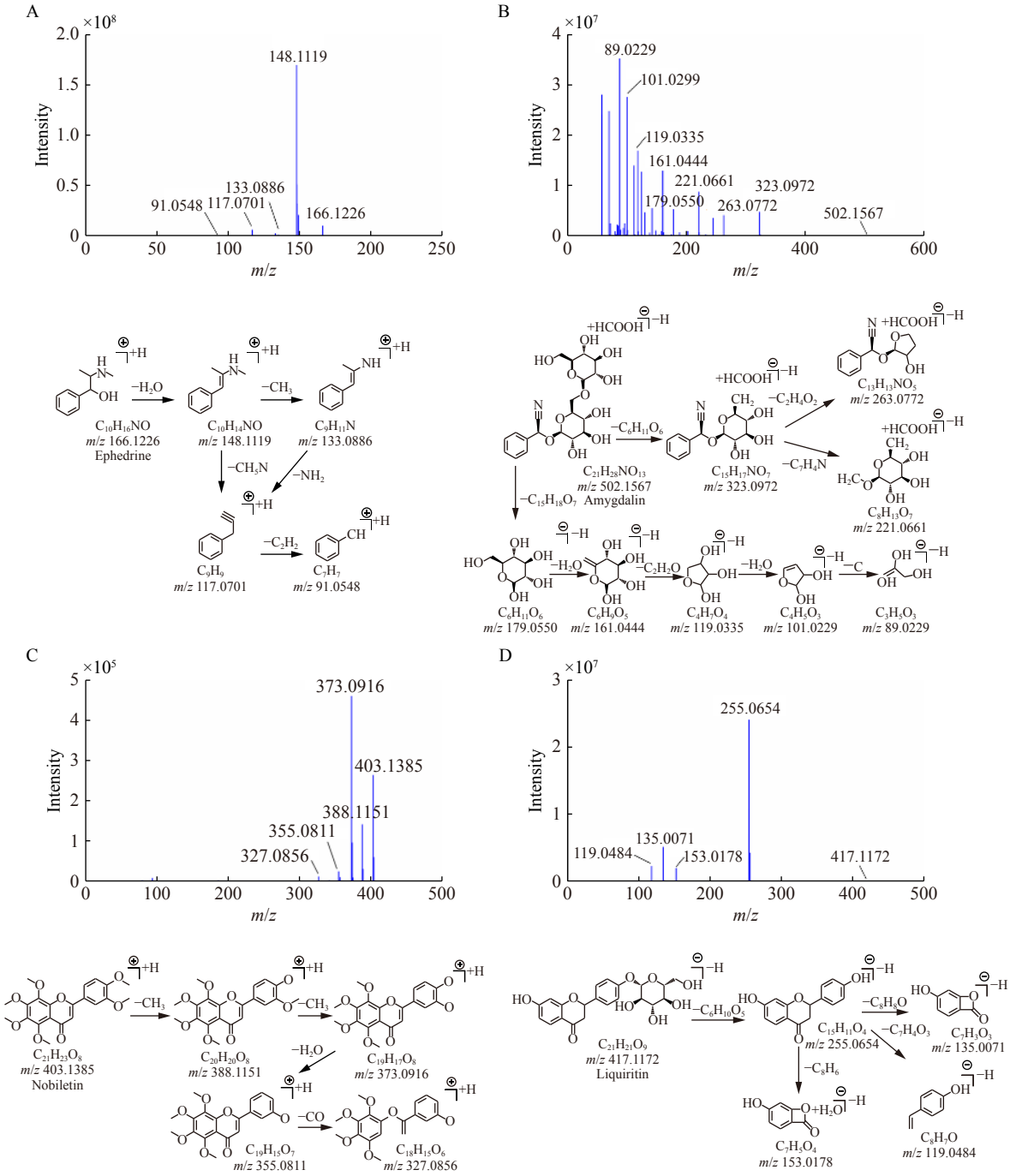

Fig. 2 The mass fragment and fragmentation pathway of ephedrine (A), amygdalin (B), nobiletin (C) and liquiritin (D)

MS/MS fragmentation analysis demonstrated that this natural compound possessed demethylation, dehydration, and CO, evidenced by the product ions of *m/z* 388.1151 $[M + H - CH_3]^+$, 373.0916 $[M + H - CH_3 - CH_3]+$, 355.0811 $[M + H - 2CH_3 - H_2O]^+$ and 327.0856 $[M + H - 2CH_3 - H_2O - CO]^+$ (Fig. 2C). The compound **321** listed in Supplementary Table S1 were detected in the positive ion mode at 29.30 min with the identical *m/z* of 403.1382 ($C_{21}H_{23}O_8$), thus this peak was characterized as nobiletin. Liquiritin (t_R = 18.59 min), a flavonoid glycoside distributed in *Radix Glycyrrhizae Praeparata*, which was detected in the negative ion mode with a quasi-molecular ion $[M - H]^-$ at *m/z* of 417.1172 ($C_{21}H_{21}O_9$). Its MS/MS data were shown as *m/z* of 255.0654 $[M - H - C_6H_{10}O_5]^-$, 153.0178 $[M - H - C_6H_{10}O_5 - C_8H_6]^-$, 135.0071 $[M - H - C_6H_{10}O_5 - C_8H_8O]^-$ and 119.0484 $[M - H - C_6H_{10}O_5 - C_7H_4O_3]^-$ (Fig. 2D). The compound **135** listed in Supplementary Table S1 could be easily detected in the negative ion mode with the same t_R (at 18.59 min) and the identical *m/z* of 417.1195 ($C_{21}H_{21}O_9$), this peak was then characterized as liquiritin. Similar to the identification pro-

cess above, a total of 162 flavonoids were identified from QFPDD, including isoliquiritin, neoliquiritin, kaempferol, luteolin, quercetin, rutin, hesperidin, neohesperidin, formononetin, isoflavin, formononetin et al.

Gallic acid (t_R = 2.09 min), an organic acid distributed in a variety of herbs, which was detected in the negative ion mode with a quasi-molecular ion $[M - H]^-$ at the *m/z* of 169.0127 ($C_7H_5O_5$). MS/MS fragmentation analysis demonstrated that this natural compound possessed neutral loss of H_2O, CO_2 and/or CO (Fig. 3A), evidenced by the product ions of *m/z* 151.0020 $[M - H - H_2O]^-$, 125.0226 $[M - H - CO_2]^-$, 97.0277 $[M - H - CO_2 - CO]^-$, 81.0327 $[M - H - 2CO_2]^-$ and 69.0327 $[M - H - CO_2 - 2CO]^-$. Compound **40** listed in Supplementary Table S1 could be detected in the negative ion mode with the same t_R (at 2.09 min) and the identical *m/z* of 169.0133 ($C_7H_5O_5$), this compound was then characterized as gallic acid. Chlorogenic acid (t_R = 12.51 min), an organic acid which was produced from caffeic acid and quinic acid, it was distributed in variety of herbs. It could be easily detected in the positive ion mode with a quasi-molecular ion $[M - H]^-$ at *m/z* 353.0883 ($C_{16}H_{17}O_9$). MS/MS fragmentation analysis demonstrated that it was easily broken down into caffeic acid and quinic acid to generate base peak ions *m/z* of 191.0549 $[M - H - C_9H_6O_3]^-$ and 179.0337 $[M -$

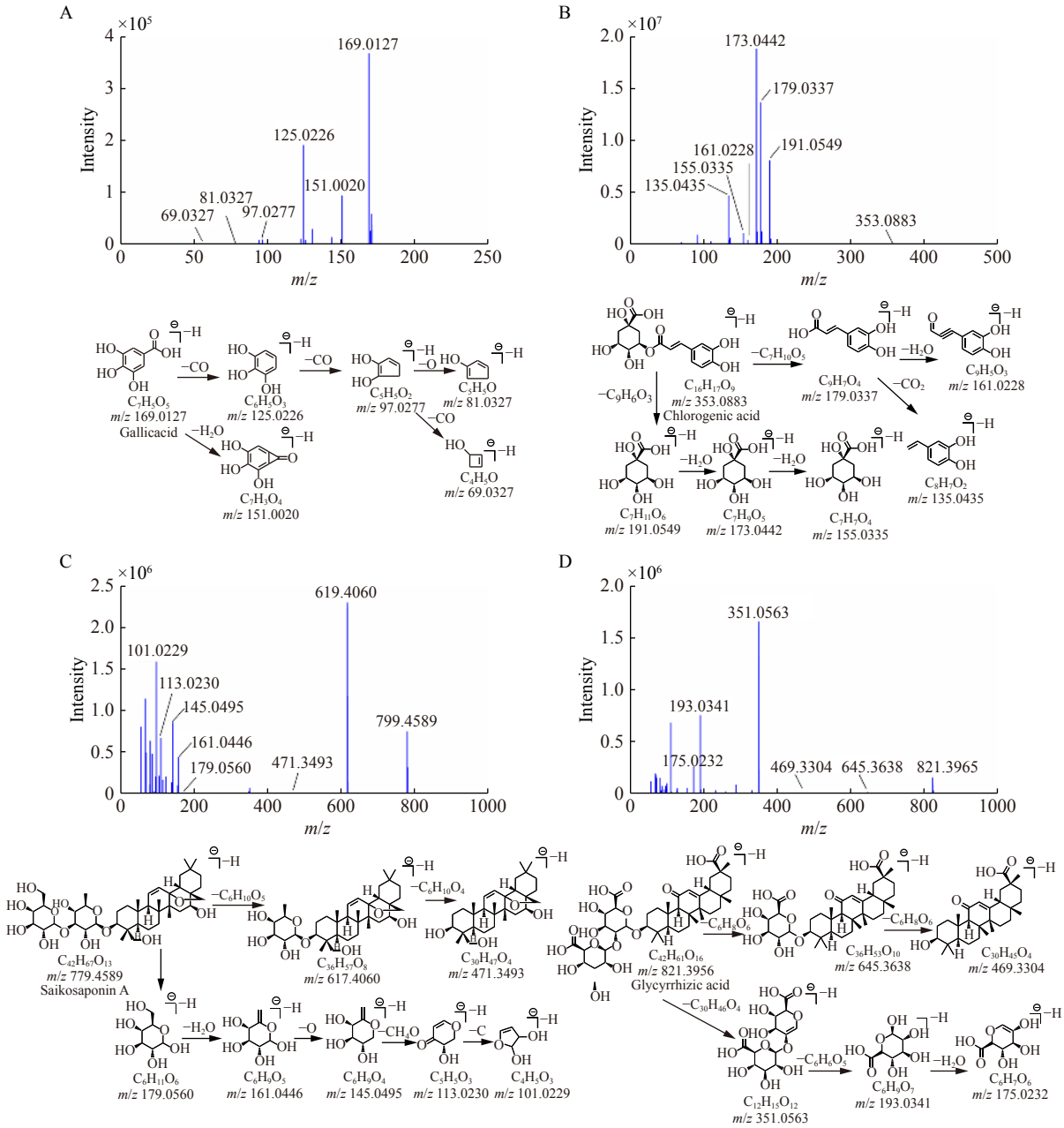

Fig. 3 The mass fragment and fragmentation pathway of gallic acid (A), chlorogenic acid (B), saikosaponin A (C) and glycyrrhizic acid (D)

H − $C_7H_{10}O_5$]$^-$ in MS^2 spectra (Fig. 3B). Subsequently by neutral loss of H_2O or CO_2, evidenced by the product ions of *m/z* 173.0442 [M − H − $C_9H_6O_3$ − H_2O]$^-$, 161.0228 [M − H − $C_7H_{10}O_5$ − H_2O]$^-$, 155.0335 [M − H − $C_9H_6O_3$ − $2H_2O$]$^-$ and 135.0435 [M − H − $C_7H_{10}O_5$ − CO_2]$^-$. Compound **81** listed in Supplementary Table S1 could be easily detected in the negative ion mode with the same Rt (at 12.51 min) and the identical *m/z* of 353.0880 ($C_{16}H_{17}O_9$), thus this compound was characterized as chlorogenic acid. Similar to the identification process above, a total of 44 organic acids were identified from QFPDD, including tartaric acid, quinic acid, citric acid, succinic acid, caffeic acid, vanillic acid isochlorogenic acid A, isochlorogenic acid B, isochlorogenic acid C, coumaroyltartaric acid, et al.

Saikosaponin A (t_R = 33.42 min), a triterpene saponins distributed in *Radix Bupleuri*, could be easily detected in the negative ion mode with a quasi-molecular ion [M − H]$^-$ at *m/z* 779.4589 ($C_{42}H_{67}O_{13}$). It was inclined to lose the sugar moiety to generate base peak ions *m/z* of 617.4060 [M − H − $C_6H_{10}O_5$]$^-$, 471.3493 [M − H − $C_6H_{10}O_5$ − $C_6H_{10}O_4$]$^-$ and 179.0560 [$C_6H_{11}O_6$]$^-$ in MS^2 spectra (Fig. 3C). Simultaneously the fragmentation signal of glucose was detected, its MS/MS data were shown as *m/z* of 161.0446 [$C_6H_{11}O_6$ − H_2O]$^-$, 145.0495 [$C_6H_{11}O_6$ − H_2O − O]$^-$, 113.0495 [$C_6H_{11}O_6$ − H_2O − $C_2H_4O_2$]$^-$ and 101.0229 [$C_6H_{11}O_6$ − H_2O − $C_3H_4O_2$]$^-$. Compound **374** listed in Supplementary Table S1 could also be detected in the negative ion mode at the same Rt (at 33.42 min) with the *m/z* of 825.4652 ($C_{42}H_{67}O_{13}$), thus this compound was characterized as saikosaponin A. Glycyrrhizic acid (t_R = 31.86 min), a triterpene saponins distributed in *Radix Glycyrrhizae Praeparata*, could be detected in the negative ion mode with a quasi-molecular ion [M − H]$^-$ at *m/z* of 821.3956 ($C_{42}H_{61}O_{16}$) in Fig. 3D. MS/MS fragmentation analysis demonstrated that this natural compound possessed loss of glucuronic acid group and glucosyl group, evidenced by the product ions of *m/z* 645.3638 [M − H − $C_6H_8O_6$]$^-$, 469.3304 [M − H − $C_6H_8O_6$ − $C_6H_8O_6$]$^-$. Simultaneously the fragmentation signal of glucuronic acid group and glucosyl group was detected, its MS/MS data were shown as *m/z* of 351.0563 [M − H − $C_{30}H_{46}O_4$]$^-$, 193.0341 [M − H − $C_{30}H_{46}O_4$ − $C_6H_6O_5$]$^-$ and 175.0232 [M − H − $C_{30}H_{46}O_4$ − $C_6H_6O_5$ − H_2O]$^-$. Compound **355** listed in Supplementary Table S1 could also be detected in the negative ion mode at the same t_R (31.86 min) with the identical *m/z* of 821.3973 ($C_{42}H_{61}O_{16}$) and fragment ions, thus this compound was characterized as glycyrrhizic acid. Similar to the identification process above, a total of 71 triterpene saponins were identified from QFPDD, including saikosaponin B2, saikosaponin C, saikosaponin D, saikosaponin F, saikosaponin M, licorice saponin A3, licorice saponin B2, licorice Saponin G2, alisol A, alisol B, alisol C, alisol O, alisol A-23-acetate, alisol B-23-acetate, et al.

The remaining 88 kinds of chemical constituents were identified from QFPDD, including amino acids, nucleosides, sugars, phenols et al. they were tentatively characterized based on their retention times and mass spectrometric data, referring to the reference standards and previous literature. For example, MS^2 spectra of compound **203** (molecular ion at *m/z* [M + H]$^+$ 133.0647) in Supplementary Table S1 showed several characteristic fragment ions of *m/z* 115.0538 [M + H − H_2O]$^+$, *m/z* 105.0673 [M + H − CO]$^+$, *m/z* 86.1003[M + H − H_2O − C_2H_5]$^+$. Thus, it corresponded to cinnamaldehyde by comparison with authentic standards and literature data [25]. Moreover, MS^2 spectra of compound **322** (molecular ion at *m/z* [M + H]$^+$ 285.0752) in Supplementary Table S1 gave characteristic fragment ions of *m/z* 270.0912 [M + H − CH_3]$^+$, *m/z* 254.0943 [M + H − CH_3O]$^+$, *m/z* 253.0897 [M + H − CH_3 − OH]$^+$ and *m/z* 225.0911 [M + H − CH_3O − CHO]$^+$. Then it was identified as batatasin I by comparison with authentic standards and literature data [26].

Characterization of the absorbed chemical constituents (prototype and metabolites) in mice serum

Next, the serum samples collected from QFPDD-treated mice at different sampling times (1, 2 and 4 h) were analyzed by UHPLC-Q-Exactive-Orbitrap HRMS to observe the peak numbers and their response in TIC chromatograms. It was found that more peaks could be detected from 1 h serum samples, suggesting that most absorbed prototype constituents or metabolite could be detected in this sample. Thus, the serum samples collected from QFPDD-treated mice at 1 h were collected and mixed for LC-MS analysis to detect the absorbed prototypes and metabolites as more as possible. With the help of the key information of the constituents in QFPDD (as listed in Supplementary Table S1), a total of 104 prototype compounds were presumed, including 12 kinds of alkaloids, 55 kinds of flavonoids, 21 kinds of organic acids, 8 kinds of triterpene saponins and 8 kinds of other compounds (Supplementary Table S2, Fig. 4 and Fig. 5). Among them, 44 ingredients are confirmed by comparison with the reference standards. Take compound **p9** for example, this peak generated quasi-molecular ion [M + H]$^+$ at *m/z* 166.1225, along with characteristic fragment ions at *m/z* 148.1117 [M+H-H_2O]$^+$, 133.0879 [M + H − H_2O − CH_3]$^+$, 117.0699 [M + H − H_2O − CH_5N]$^+$ and 91.0545 [M + H − H_2O − CH_5N − C_2H_2]$^+$, which was identical to the compound **62** in the extract of QFPDD (Supplementary Table S1). Compound **p9** was thus identified as pseudoephedrine. Similarly, compound **p21** generated deprotonated molecule [M − H]$^-$ at *m/z* 294.0988, along with characteristic fragment ions at *m/z* 161.0445 [$C_6H_9O_5$]$^-$, 101.0229 [$C_6H_9O_5$ − $C_2H_4O_2$]$^-$, 85.0279 [$C_6H_9O_5$−$C_2H_4O_3$]$^-$,71.0123[$C_6H_9O_5$−$C_2H_4O_2$−CH_2O]$^-$,which was identical to the product ions of compound **93** in QFPDD. Thus, compound **p21** was characterized as prunasin.

Flavonoids were major constituents in several herbs for preparing QFPDD, it is necessary to identify the absorbed flavonoids in serum from QFPDD-treated mice. In this study, a total of 54 flavonoids (as the absorbed prototype constituents) were detected in mice serum. Take compound **p87** for example, this peak generated a quasi-molecular ion [M + H]$^+$ at *m/z* 387.1073, along with characteristic fragment ions at

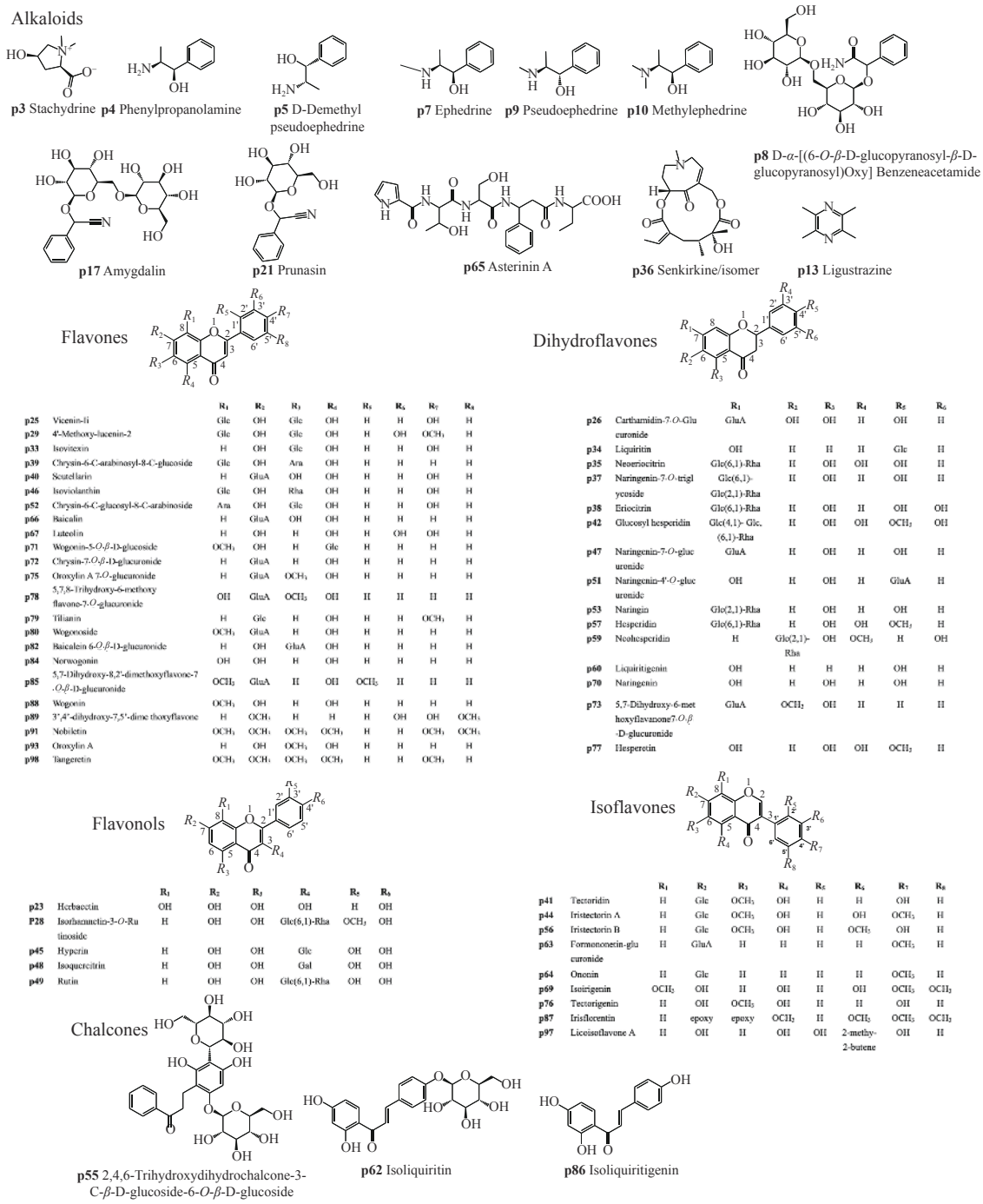

		R_1	R_2	R_3	R_4	R_5	R_6	R_7	R_8
p25	Vicenin-Ii	Glc	OH	Glc	OH	H	H	OH	H
p29	4'-Methoxy-lucenin-2	Glc	OH	Glc	OH	H	OH	OCH_3	H
p33	Isovitexin	H	OH	Glc	OH	H	H	OH	H
p39	Chrysin-6-*C*-arabinosyl-8-*C*-glucoside	Glc	OH	Ara	OH	H	H	H	H
p40	Scutellarin	H	GluA	OH	OH	H	H	OH	H
p46	Isoviolanthin	Glc	OH	Rha	OH	H	H	OH	H
p52	Chrysin-6-*C*-glucosyl-8-*C*-arabinoside	Ara	OH	Glc	OH	H	H	OH	H
p66	Baicalin	H	GluA	OH	OH	H	H	H	H
p67	Luteolin	H	OH	H	OH	H	OH	OH	H
p71	Wogonin-5-*O*-β-D-glucoside	OCH_3	OH	H	Glc	H	H	H	H
p72	Chrysin-7-*O*-β-D-glucuronide	H	GluA	H	OH	H	H	H	H
p75	Oroxylin A 7-*O*-glucuronide	H	GluA	OCH_3	OH	H	H	H	H
p78	5,7,8-Trihydroxy-6-methoxy flavone-7-*O*-glucuronide	OH	GluA	OCH_3	OH	H	H	H	H
p79	Tiliamin	H	Glc	H	OH	H	H	OCH_3	H
p80	Wogonoside	OCH_3	GluA	H	OH	H	H	H	H
p82	Baicalein 6-*O*-β-D-glucuronide	H	OH	GluA	OH	H	H	H	H
p84	Norwogonin	OH	OH	H	OH	H	H	H	H
p85	5,7-Dihydroxy-8,2'-dimethoxyflavone-7-*O*-β-D-glucuronide	OCH_3	GluA	H	OH	OCH_3	H	H	H
p88	Wogonin	OCH_3	OH	H	OH	H	H	H	H
p89	3',4'-dihydroxy-7,5'-dime thoxyflavone	H	OCH_3	H	H	H	OH	OH	OCH_3
p91	Nobiletin	OCH_3	OCH_3	OCH_3	OCH_3	H	H	OCH_3	OCH_3
p93	Oroxylin A	H	OH	OCH_3	OH	H	H	H	H
p98	Tangeretin	OCH_3	OCH_3	OCH_3	OCH_3	H	H	OCH_3	H

		R_1	R_2	R_3	R_4	R_5	R_6
p26	Carthamidin-7-*O*-Glu curonide	GluA	OH	OH	H	OH	H
p34	Liquiritin	OH	H	H	H	Glc	H
p35	Neoeriocitrin	Glc(6,1)-Rha	H	OH	OH	OH	H
p37	Naringenin-7-*O*-trigl ycoside	Glc(6,1)-Glc(2,1)-Rha	H	OH	H	OH	H
p38	Eriocitrin	Glc(6,1)-Rha	H	OH	H	OH	OH
p42	Glucosyl hesperidin	Glc(4,1)- Glc, (6,1)-Rha	H	OH	OH	OCH_3	OH
p47	Naringenin-7-*O*-gluc uronide	GluA	H	OH	H	OH	H
p51	Naringenin-4'-*O*-gluc uronide	OH	H	OH	H	GluA	H
p53	Naringin	Glc(2,1)-Rha	H	OH	H	OH	H
p57	Hesperidin	Glc(6,1)-Rha	H	OH	OH	OCH_3	H
p59	Neohesperidin	H	Glc(2,1)-Rha	OH	OCH_3	H	OH
p60	Liquiritigenin	OH	H	H	H	OH	H
p70	Naringenin	OH	H	OH	H	OH	H
p73	5,7-Dihydroxy-6-met hoxyflavanone7-*O*-β-D-glucuronide	GluA	OCH_3	OH	H	H	H
p77	Hesperetin	OH	H	OH	OH	OCH_3	H

		R_1	R_2	R_3	R_4	R_5	R_6
p23	Herbacetin	OH	OH	OH	OH	H	OH
P28	Isorhamnetin-3-*O*-Rutinoside	H	OH	OH	Glc(6,1)-Rha	OCH_3	OH
p45	Hyperin	H	OH	OH	Glc	OH	OH
p48	Isoquercitrin	H	OH	OH	Gal	OH	OH
p49	Rutin	H	OH	OH	Glc(6,1)-Rha	OH	OH

		R_1	R_2	R_3	R_4	R_5	R_6	R_7	R_8
p41	Tectoridin	H	Glc	OCH_3	OH	H	H	OH	H
p44	Iristectorin A	H	Glc	OCH_3	OH	H	OH	OCH_3	H
p56	Iristectorin B	H	Glc	OCH_3	OH	H	OCH_3	OH	H
p63	Formononetin-glu curonide	H	GluA	H	H	H	H	OCH_3	H
p64	Ononin	H	Glc	H	H	H	H	OCH_3	H
p69	Isoirigenin	OCH_3	OH	H	OH	H	OH	OCH_3	OCH_3
p76	Tectorigenin	H	OH	OCH_3	OH	H	H	OH	H
p87	Irisflorentin	H	epoxy	epoxy	OCH_3	H	OCH_3	OCH_3	OCH_3
p97	Liceisoflavone A	H	OH	H	OH	OH	2-methy-2-butene	OH	H

Fig. 4 Structures of the absorbed prototype compounds (alkaloids and flavonoids) in mice serum after oral administration of Qing-Fei-Pai-Du decoction

m/z 372.0831 $[M + H - CH_3]^+$, 357.0619 $[M + H - CH_3 - CH_3]^+$, 341.0747 $[M + H - CH_3 - CH_3O]^+$, 326.0788 $[M + H - CH_3 - CH_2O_2]^+$, which was highly consistent with the product ions of compound **302** in QFPDD. As a result, compound **p87** was identified as the prototype of compound **302** (irisflorentin). Similarly, compound **p57** shared analogical elution time and identical ions in MS^2 spectra with compound **189** in the extract of QFPDD, such as *m/z* 301.0721 $[M - H - C_{12}H_{20}O_9]^-$, 286.0478 $[M - H - C_{12}H_{20}O_9 - CH_3]^-$, 257.0801 $[M - H - C_{12}H_{20}O_9 - CO_2]^-$, 242.0597 $[M - H - C_{12}H_{20}O_9 - CH_3 - CO_2]^-$. For this reason, compound **p57** was then deemed to be hesperidin, *i.e.*, the prototype of compound **189**.

Triterpene saponins were another major group of bioactive components in QFPDD, and it was found that the majority of them could be absorbed into serum. For example, compound **p103** gave molecular formula $C_{30}H_{50}O_5$ and deprotonated molecule at *m/z* 535.3648 $[M + FA - H]^-$, along with

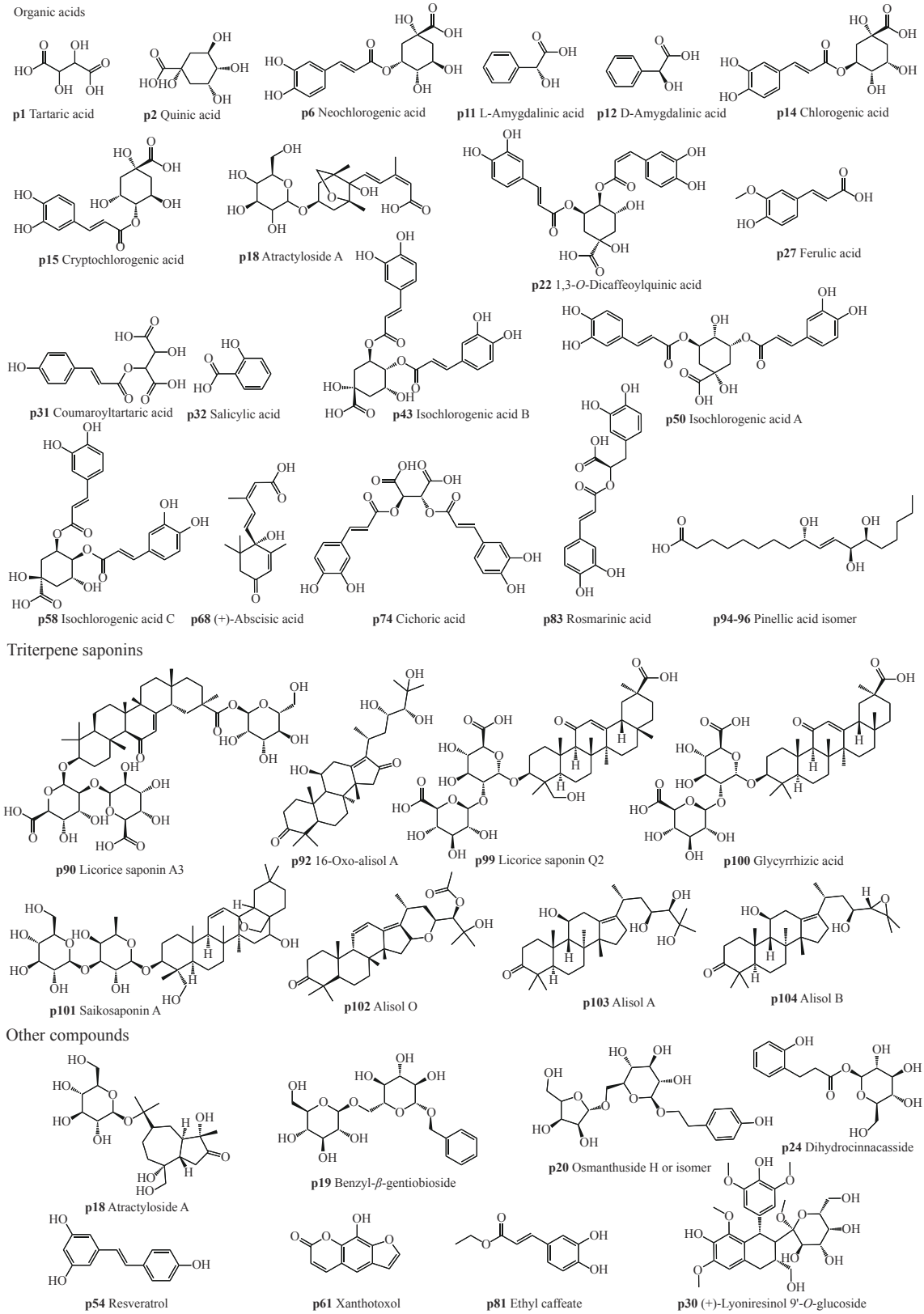

Fig. 5 Structures of the absorbed prototype compounds (organic acids, triterpene saponins, and others) in mice serum after oral administration of Qing-Fei-Pai-Du decoction

distinctive fragment ions at *m*/*z* generated deprotonated molecule $[M + FA - H]^-$ at *m*/*z* 471.3481 $[M - H - H_2O]^-$, 395.2949 $[M - H - H_2O - C_3H_8O_2]^-$, 371.2598 $[M - H - H_2O - C_6H_{12}O]^-$, 353.2497 $[M - H - H_2O - C_6H_{12}O -$

$H_2O]^-$, which was in keeping with compound **396** in the extract of QFPDD. Then, compound **p103** was regarded as prototype of compound **396**.

Similarly, compound **p50** (an organic acid) occurring in rat serum showed identical retention times and quasi-molecular ion (*m/z* 515.1202 $[M - H]^-$) to compound **158** in QFPDD. Furthermore, they also produced near identical fragment ions in MS^2 spectra, *e.g.*, *m/z* *m/z* 353.0884 $[M - H - C_9H_6O_3]^-$, 191.0554 $[M - H - C_9H_6O_3 - C_9H_6O_3]^-$, 179.0337 $[M - H - C_9H_7O_4 - C_9H_7O_4]^-$, 161.0234 $[M - H - C_9H_6O_3 - C_7H_{13}O_5]^-$. Thus, compound **p50** was identified as the prototype of compound **158**, namely isochlorogenic acid A.

Identification of the metabolites in mice serum

Next, the metabolites in serum from QFPDD-treated mice that are derived from the constituents in QFPDD were tentatively characterized. To discriminate the endogenous metabolites from QFPDD-related metabolites, the TIC chromatograms of QFPDD-treated mice serum were compared with that of the blank serum. After then, the endogenous substances could be excluded, while the exogenous compounds could be identified by comprehensive analysis. By contrasting these compounds with already known compounds *in vitro*, searching for the same compounds and validating them *via* comparison of the retention time and the product ions. TraceFinder software incorporated in UHPLC-Q-Exactive-Orbitrap HRMS could process the data acquired, provide key information about group changes from prototypes to metabolites by means of exact molecular weight, and provide elementary compositions thereof. These analyses were beneficial to determine the prototypes and the metabolites in biological samples, and to conjecture potential metabolic pathways. Furthermore, in this study, parts of *in vivo* metabolites of the major constituents in QFPDD were identified *via* comparison with the retention times and MS/MS spectra of the *in vitro* metabolites generated in MLMs.

Taking metabolites **M27**, **M30** and **M65** as the examples, these three compounds gave similar quasi-molecular ion $[M - H]^-$ at *m/z* 431.0983, as well as characteristic fragment ions at *m/z* 255.0665 [−176 Da, $M - H - C_6H_8O_6]^-$, *m/z* 135.0090 $[M - H - C_6H_8O_6 - C_8H_8O]^-$, *m/z* 119.0501 $[M - H - C_6H_8O_6 - C_7H_4O_3]^-$ in the MS^2 spectrum. The fragment ions of these three metabolites were identical with that of compound **205** (liquiritigenin), a major constituent identified from the extract of QFPDD. *In vitro* metabolism of liquiritigenin in MLMs incubated with both NADPH and UDPGA, three mono-*O*-glucuronides could be easily detected. The retention times, product ions were consistent with the metabolites **M27, M30** and **M65**. In these cases, these three compounds were identified as liquiritigenin-*O*-glucuronide. Similarly, the *in vivo* metabolites **M34** and **M70** are identified as typical sulfates, both compounds displayed similar quasi-molecular ion $[M - H]^-$ at *m/z* 335.0231, as well as characteristic fragment ions at *m/z* 255.0665 [−80 Da, $M - H - SO_3]^-$, *m/z* 135.0090 $[M - H - SO_3 - C_8H_8O]^-$, *m/z* 119.0501 $[M - H - SO_3 - C_7H_4O_3]^-$ in the MS^2 spectrum, the fragment ions were identical with that of the authentic standard liquiritigenin. *In vitro* metabolism demonstrated that following incubation of liquiritigenin in MLMs in the presence of both NADPH and PAPS, two mono-*O*-sulfates could be easily detected. The retention times, product ions were well-matched with the metabolites **M34** and **M70**. Thus, these two peaks were identified as liquiritigenin-*O*-sulfate.

The metabolite **M21** and **M25** were produced from an organic acid. They gave similar quasi-molecular ion $[M - H]^-$ at *m/z* 367.1034, as well as characteristic fragment ions at *m/z* 353.0883 [−15 Da, $M - H - CH_3]^-$, *m/z* 191.0549 $[M - H - CH_3 - C_9H_6O_3]^-$, *m/z* 179.0337 $[M - H - CH_3 - C_7H_{10}O_5]^-$, *m/z* 173.0442 $[M - H - C_9H_6O_3 - H_2O]^-$, *m/z* 161.0228 $[M - H - CH_3 - C_7H_{10}O_5 - H_2O]^-$ in the MS^2 spectrum, the fragment ions were identical with the compound **59** (neochlorogenic acid), **80** (chlorogenic acid), **87** (cryptochlorogenic acid) in the extract of QFPDD. *In vitro* metabolism demonstrated that following incubation of chlorogenic acid in MLMs in the presence of NADPH and SAM, two *O*-methylated metabolites were detected. The retention times, product ions were well-matched with that of the metabolites **M21** and **M25**. Thus, these two metabolites were identified as *O*-methylated chlorogenic acid. Previous study have reported that two *O*-methylated metabolites of chlorogenic acid were found in urine samples after intramuscular administration of chlorogenic acid injection to healthy adults, and the pure *O*-methylated metabolites were synthesized by chlorogenic acid and followed by isolation, purification and identification [27]. According to the chromatographic behavior of them, **M21** was tentatively identified as 3′- methyl-chlorogenic acid, and **M25** was tentatively identified as 4′- methyl-chlorogenic acid.

Following carefully metabolite identification as mentioned above, a total of 91 metabolites were tentatively identified (Supplementary Table S3). A variety of metabolic reactions, such as hydroxylation, *O*-methylation, *O*-glucuronidation, *O*-sulfation, demethylation, were involved in the metabolism of the major constituents in QFPDD. Among them, 20 metabolites are fully confirmed by the *in vitro* metabolites generated in MLM.

Characterization of the absorbed prototypes and metabolites in mice tissues

With the help of the information about the absorbed prototypes and metabolites in mice serum, the absorbed prototypes and metabolites in various tissues from QFPDD-treated mice were explored. Subsequently, total of 165, 177, 112, 120, 44 and 53 prototypes and metabolites were identified in the lung, liver, heart, kidney, brain, and spleen of QFPDD-treated mice, respectively. The peak areas of absorbed prototypes and metabolites were summarized in Supplementary Table S2 and Supplementary Table S3, while Fig. 6 showed the heat map of the peak areas of both the absorbed components and the metabolites occurring in serum or six different

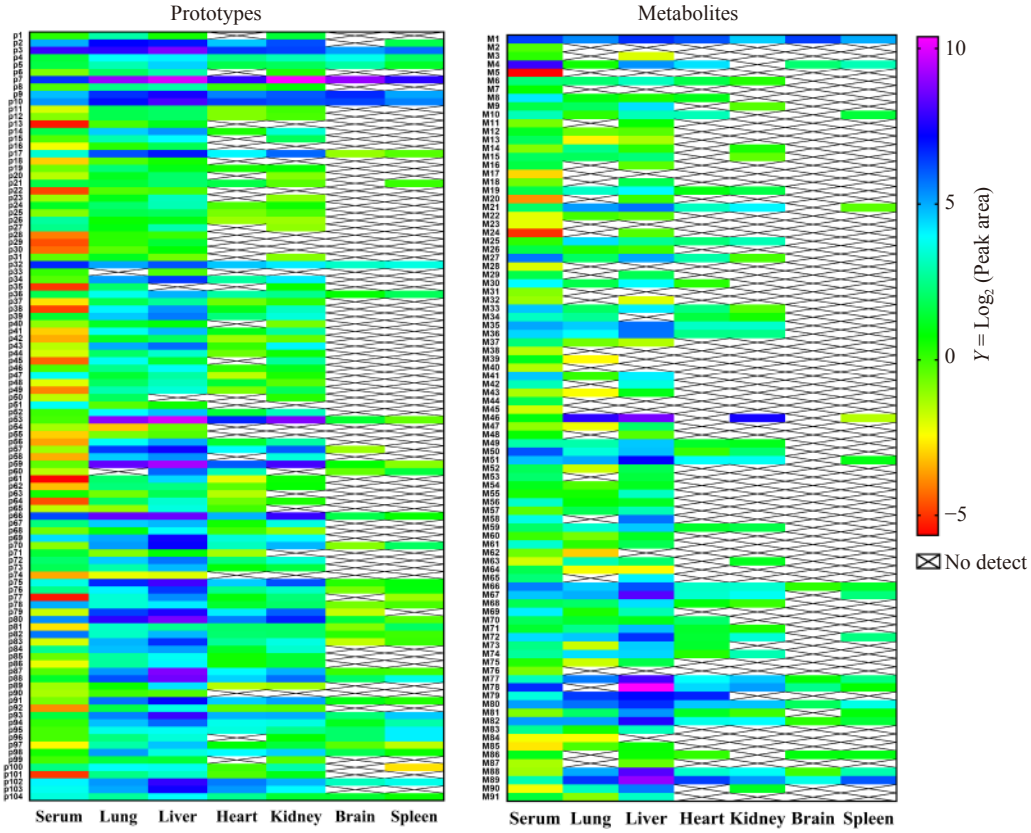

Fig. 6 The heat map of the peak areas of absorbed components and metabolites in mice serum and tissues after oral administration Qing-Fei-Pai-Du decoction

tissues of QFPDD-treated mice.

On the basis of the peak area, the top ten components in the mice serum were ranked as follows, stachydrine (**p3**), salicylic acid (**p32**), ephedrine (**p7**), caffeic acid-sulfate (**M4**), baicalin (**p66**), baicalein 6-*O*-β-D-glucuronide (**p82**), wogonoside (**p80**), methylephedrine (**p10**), baicalein-glucuronide methylation (**M78**), quinic acid (**p2**).

The top ten components in the lung tissue were ranked as follows: ephedrine (**p7**), naringin (**p53**), neohesperidin (**p59**), baicalin (**p66**), wogonoside (**p80**), stachydrine (**p3**), quinic acid (**p2**), methylephedrine (**p10**), oroxylin A 7-*O*-glucuronide (**p75**), pseudoephedrine (**p9**).

The top ten components in the liver tissue were ranked as follows: ephedrine (**p7**), naringin (**p53**), neohesperidin (**p59**), baicalein-glucuronide methylation (**M78**), irisflorentin (**p87**), stachydrine (**p3**), wogonoside (**p80**), wogonin (**p88**), baicalin (**p66**), methylephedrine (**p10**).

The top ten components in the heart tissue were ranked as follows: ephedrine (**p7**), naringin (**p53**), stachydrine (**p3**), methylephedrine (**p10**), neohesperidin (**p59**), alisol O (**p102**), wogonoside (**p80**), pseudoephedrine (**p9**), baicalein-methoxylation (**M79**), alisol A (**p103**).

The top ten components in the kidney tissue were ranked as follows: ephedrine (**p7**), naringin (**p53**), neohesperidin (**p59**), baicalin (**p66**), wogonoside (**p80**), stachydrine (**p3**), methylephedrine (**p10**), quinic acid (**p2**), oroxylin A 7-*O*-glucuronide (**p75**), pseudoephedrine (**p9**).

The top ten components in the brain tissue were ranked as follows: ephedrine (**p7**), pseudoephedrine (**p9**), methylephedrine (**p10**), stachydrine (**p3**), mandelonitrile (**M1**), phenylpropanolamine (**p4**), salicylic acid (**p32**), alisol O (**p102**), D-demethyl pseudoephedrine (**p5**), oroxylin A (**p93**).

The top ten components in the spleen tissue were ranked as follows: ephedrine (**p7**), stachydrine (**p3**), methylephedrine (**p10**), pseudoephedrine (**p9**), oroxylin A (**p93**), baicalein -methoxylation (**M89**), pinellic acid isomer (**p96**), alisol O (**p102**), wogonin (**p88**).

From the above results, it was obvious that ephedrine (**p7**) and methylephedrine (**p10**) from *Herba Ephedrae*, and stachydrine (**p3**) from *Fructus Aurantii Immaturus* displayed relatively high exposure levels in mice serum and all tested tissues. Additionally, baicalin (**p66**), oroxylin A 7-*O*-glucuronide (**p75**), wogonoside (**p80**), wogonin (**p88**) and oroxylin A (**p93**) from Radix Scutellariae, alisol O (**p102**) and alisol A (**p103**) from Rhizoma Alismatis also showed relatively high exposure levels in most of mice tissues.

Discussion

To fight against COVID-19, some Chinese medicines were recommended by National Health Commission of the People's Republic of China or the local government in China, for alleviating the major symptoms of COVID-19 or prevent-

ing disease deterioration [10]. As the first Chinese medicine compound formula recommended for combating COVID-19, QFPDD is made by 20 herbs and a mineral drug, which is composed by hundreds of ingredients. In most cases, for treating COVID-19, the absorbed constituents (including the prototypes and the metabolites) into blood circulation can be delivered to the target organ (such as the lung) and then exerts various pharmacological effects, such as anti-inflammatory and anticoagulant effects [28, 29]. Therefore, it is necessary to investigate the absorbed constituents of QFPDD following oral administration of this super Chinese medicine compound formula, which will be very helpful for better understanding the key material basis of QFPDD, as well as for guiding the quality control and clinical applications of this formula.

In this study, an UHPLC-Q-Orbitrap HRMS based method was established for profiling the constituents in QFPDD and the absorbed constituents in QFPDD-treated mice. The research strategy and the key findings for clarifying the chemical composition and absorption components of QFPDD have been summarized in Fig. 7. The chemical constituents in QFPDD were tentatively identified *via* comparison with exact molecular weight, the retention times and MS/MS spectra of the standards or refereed by TCM databases and literature. The absorbed components (including the prototypes and the metabolites) occurring in mice serum and tissues were identified *via* profiling the serum and tissue samples from QFPDD-treated mice. The absorbed prototype components were tentatively identified *via* comparison with the retention times and MS/MS spectra of components in QFPDD. The *in vivo* metabolites were tentatively identified *via* comparison with fragment ions of the parent compounds or refereed by literature, while parts of *in vivo* metabolites of the major constituents were identified *via* comparison with the retention times and MS/MS spectra of the *in vitro* metabolites of each constituent generated in MLMs. Finally, a total of 405 chemicals (including alkaloids, flavonoids, organic acids, triterpene saponins and other compounds) in the extract of QFPDD were identified, while 195, 165, 177, 112, 120, 44, 53 constituents were identified in the serum, lung, liver, heart, kidney, brain, and spleen of QFPDD-treated mice, respectively. All these findings might be very helpful for deep understanding the fates of the constituents in QFPDD, as well as offered key information of the tissue distribution of the absorbed components of this anti-COVID-19 Chinese medicine.

It is well known that it is always a challenging task for identification of the prototypes and the metabolites of TCM prescription. For example, oroxylin A 7-*O*-glucuronide (**p75**) is a trace amount prototype constituent occurring in QFPDD, but this agent is a highly exposed component in the serum and various tissues of QFPDD-treated mice. The reasons may include i) produced by the *O*-glucuronidation of oroxylin A (**p103**) *in vivo*; ii) produced by baicalein (**p66**) through 6-*O*-

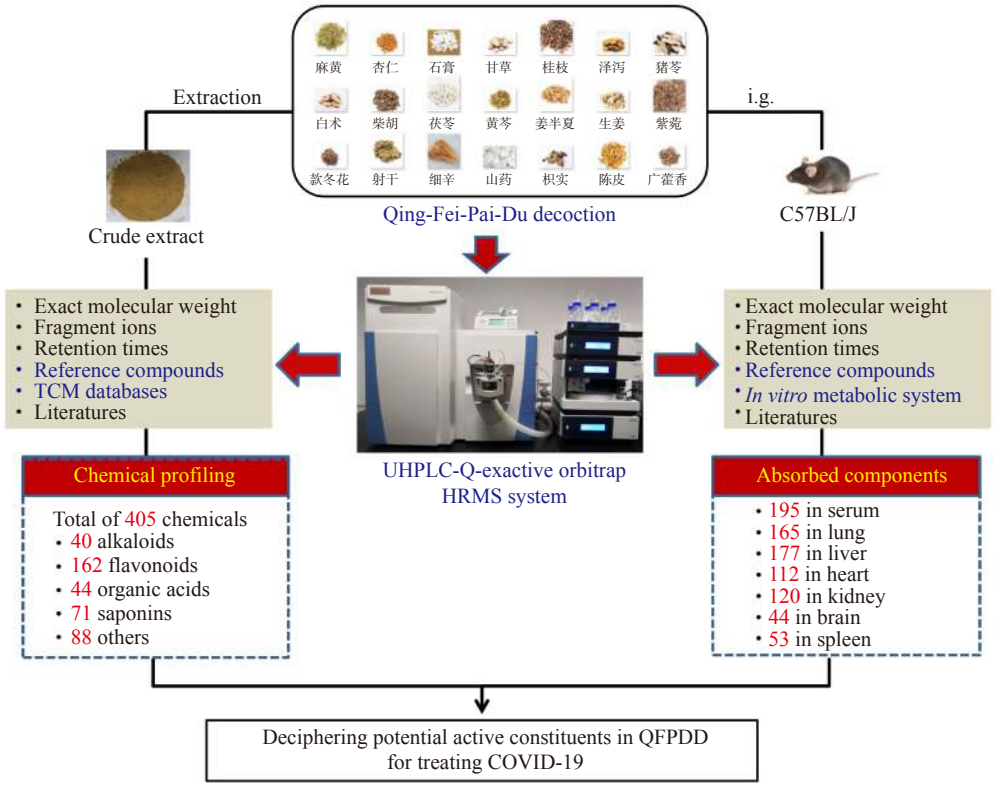

Fig. 7 Research strategy for clarifying the chemical composition and absorption components of Qing-Fei-Pai-Du decoction based on UHPLC-Q-Exactive Orbitrap HRMS technology

methylation and *O*-glucuronidation. It is also suggested that it is very difficult to differentiate some components detected in QFPDD-treated mice as the prototypes or the metabolites, owing to that some *in vivo* components are derived from both the prototypes and the metabolites of the homologous compounds occurring in this TCM prescription. Meanwhile, the exposure of some prototype constituents in blood are extremely low and thus are difficult to be detected, since these natural constituents could be readily transformed into the corresponding metabolites (glucuronides or sulfates) *in vivo*. For instances, trihydroxy-methoxyflavone-*O*-glucuronides (**M35** and **M60**) and daidzein-sulfates (**M33** and **M41**) can be easily detected in mice serum, but the related prototypes are hardly detected in mice serum. In addition, many nature products have isomers that cannot be distinguished by MS spectral analysis alone, thus it is hard to correlate the parent compounds with the metabolites, such as vanillic acid and its isomer.

Modern pharmacological studies have found that some of absorbed components of QFPDD displayed a wide range of benificical effects or biological activities. Some pharmacological activities of them are considered to be beneficial for COVID-19 patients. For example, ephedrine, pseudoephedrine and amygdalin displayed significant anti-cough and anti-asthmatic effects [30], as well as anti-inflammatory [31, 32] and immunomodulatory effects [33, 34], which are considered as the major active components of TCM prescriptions for treating respiratory diseases. Zhang et al. [35] report that amygdalin can induce LPS by inhibiting NF-κB and NLRP3 signaling pathways, while baicalin has antiviral, anti-inflammatory, antioxidant, and immunomodulatory pharmacological activities [36]. A recent study has reported that baicalin can significantly inhibit the catalytic activity of SARS-CoV-2 $3CL^{pro}$ and then exert antiviral activity [37]. The virtual screening of active ingredients of SARS-CoV-2 virus also suggests that hesperidin and baicalin have potential inhibitory effects [38]. The glycyrrhizin and glycyrrhizic acid in licorice have been found with extensive anti-inflammatory [39] and anti-damage effects [40]. Some previous studies have shown that glycyrrhizin can serve as an alternative agent for treating COVID-19 infection and its associated respiratory syndrome [41-43]. The extract of Rhizoma Alismatis processed exerts anti-inflammatory activity *via* inhibiting cytochrome P450 enzymes [44], the key enzymes responsible for the metabolism of arachidonic acid, thereby reducing the production of inflammatory factors [45-47].

Furthermore, some *in vivo* metabolites of QFPDD are more likely to be the active ingredients. Previous studies clearly demonstrated that a panel of *O*-glucuronides of flavonoids displayed good anticoagulant activities, and their anticoagulant activities are better than that of the prototypes [48]. Recent studies have shown that the blood of COVID-19 patients was in a hypercoagulable state, thus the *O*-glucuronides of flavonoids were more likely to promote blood circulation through anticoagulation and then relieve the symptoms of patients [49-51]. This study was not only found a considerable number of prototypes and metabolites in serum, but also found a large number of chemical components in lung, liver and other tissues. Among them, the active ingredients derived from *Herba Ephedrae* (ephedrine, pseudoephedrine, methylephedrine, phenylpropanolamine etc.), *Fructus Aurantii Immaturus* (stachydrine, naringin, hesperidin, neohesperidin, quinic acid etc.), *Radix Scutellariae* (baicalin, oroxylin A 7-*O*-glucuronide, wogonoside, wogonin, oroxylin A etc.) and *Rhizoma Alismatis* (alisol O, alisol A etc.) displayed relatively high exposure levels in most of tested organs. However, the kinds and exposure levels of each component in various tissues are much different. These findings suggest that these *in vivo* metabolites of QFPDD may play potential role in the treatment of COVID-19 *via* targeting multiple targets or pathways. In future, the bioactive ingredients and mechanisms of action can be explored.

Conclusion

In summary, a practical and sensitive UHPLC-Q-Exactive-Orbitrap HRMS approach was developed for chemical profiling of the constituents in QFPDD, as well as the absorbed prototypes and the metabolites in mice serum and tissues following oral administration of QFPDD. With the help of the authentic standards and *in vitro* metabolites generated by MLM, a total of 405 constituents (including 40 kinds of alkaloids, 162 kinds of flavonoids, 44 kinds of organic acids, 71 kinds of triterpene saponins and 88 kinds of other compounds) were identified from the water extract of QFPDD, while 195 components (including 104 prototypes and 91 metabolites) were identified from mice serum after oral administration of QFPDD to mice. Meanwhile, 165, 177, 112, 120, 44, 53 components were identified from the lung, liver, heart, kidney, brain, and spleen of QFPDD-treated mice, respectively. Additionally, the metabolic pathways of some major absorbed components occurring in the serum of QFPDD-treated mice were also described. All these findings provided key information and guidance for further investigations on the pharmacologically active substances and quality control of QFPDD.

Abbreviations

CMs, Chinese Medicines; COVID-19, Corona Virus Disease 2019; CYPs/P450s, cytochrome P450 enzymes; ESI, electrospray ionization; G-6-P, D-Glucose-6-phosphate; G-6-PDH, glucose-6-phosphate dehydrogenase; MLMs, mice liver microsomes; β-$NADP^+$, nicotinamide adenine dinucleotide phosphate disodium salt; PAPS, 3-phosphoadenosine 5-phosphosulfate; PBS, potassium phosphate buffer; QFPDD, Qing-Fei-Pai-Du decoction; SAM, *S*-adenosyl-L-methionine; SARS, Severe Acute Respiratory Syndrome; UDPGA, uridine di-phosphate glucuronic acid; UHPLC-Q-Orbitrap HRMS, ultra-high-performance liquid chromatography-Q exactive hybrid quadrupole orbitrap high-resolution accurate

mass spectrometric.

Acknowledgements

We thank Asso. Prof. WU Cai-Sheng from Xiamen University, for his help in identification of prototype constituents and metabolites in mice serum following oral administration of QFPDD to mice.

Supplementary Materials

Supplementary materials are available as Supporting Information, and can be requested by sending E-mail to the corresponding author.

References

[1] Hamidian Jahromi A, Hamidianjahromi A. Why African Americans are a potential target for COVID-19 infection in the United States [J]. *J Med Internet Res*, 2020, **22**: e19934.

[2] Dima M, Enatescu I, Craina M, *et al*. First neonates with severe acute respiratory syndrome coronavirus 2 infection in Romania: three case reports [J]. *Medicine (Baltimore)*, 2020, **99**: e21284.

[3] Niu S, Tian S, Lou J, *et al*. Clinical characteristics of older patients infected with COVID-19: a descriptive study [J]. *Arch Gerontol Geriatr*, 2020, **89**: 104058.

[4] Luo E, Zhang D, Luo H, *et al*. Treatment efficacy analysis of traditional Chinese medicine for novel coronavirus pneumonia (COVID-19): an empirical study from Wuhan, Hubei Province, China [J]. *Chin Med*, 2020, **15**: 34.

[5] Chen J, Wang YK, Gao Y, *et al*. Protection against COVID-19 injury by qingfei paidu decoction *via* anti-viral, anti-inflammatory activity and metabolic programming [J]. *Biomed Pharmacother*, 2020, **129**: 110281.

[6] Li H, Lu WL, Sun YN, *et al*. Real world clinical study of Chinese medicine treatment of 749 patients with coronavirus disease 2019 [J]. *Chin J Tradit Chin Med*, 2020, **35**: 3194-3198.

[7] Dai YJ, Wan SY, Gong SS, *et al*. Recent advances of traditional Chinese medicine on the prevention and treatment of COVID-19 [J]. *Chin J Nat Med*, 2020, **18**: 881-889.

[8] Ling CQ. Traditional Chinese medicine is a resource for drug discovery against 2019 novel coronavirus (SARS-CoV-2) [J]. *J Integr Med*, 2020, **18**(2): 87-88.

[9] Zhang Y, Xie H, Li Y, *et al*. Qingfei Paidu decoction for treating COVID-19: a protocol for a meta-analysis and systematic review of randomized controlled trials [J]. *Medicine (Baltimore)*, 2020, **99**: e22040.

[10] Ni L, Chen L, Huang X, *et al*. Combating COVID-19 with integrated traditional Chinese and Western medicine in China [J]. *Acta Pharm Sin B*, 2020, **10**: 1149-1162.

[11] Meng JH, He Y, Chen Q, *et al*. A retrospective study of Qingfei Paidu Decoction in the treatment of common/severe new coronavirus pneumonia [J]. *Chin J Hospit Pharm*, 2020, **40**(20): 2152-2157.

[12] Xin S, Cheng X, Zhu B, *et al*. Clinical retrospective study on the efficacy of Qingfei Paidu Decoction combined with western medicine for COVID-19 treatment [J]. *Biomed Pharmacother*, 2020, **129**: 110500.

[13] Yang R, Liu H, Bai C, *et al*. Chemical composition and pharmacological mechanism of Qingfei Paidu Decoction and Ma Xing Shi Gan Decoction against Coronavirus Disease 2019 (COVID-19): in silico and experimental study [J]. *Pharmacol Res*, 2020, **157**: 104820.

[14] Shi NN, Liu B, Liang N, *et al*. Association between early treatment with Qingfei Paidu decoction and favorable clinical outcomes in patients with COVID-19: a retrospective multicenter cohort study [J]. *Pharmacol Res*, 2020, **161**: 105290.

[15] Ge GB. Deciphering the metabolic fates of herbal constituents and the interactions of herbs with human metabolic system [J]. *Chin J Nat Med*, 2019, **17**: 801-802.

[16] Zhou QH, Zhu YD, Zhang F, *et al*. Interactions of drug-metabolizing enzymes with the Chinese herb Psoraleae Fructus [J]. *Chin J Nat Med*, 2019, **17**: 858-870.

[17] Li CH. Analysis of Qingfei Paidu Decoction in the treatment of new coronavirus pneumonia [J]. *Chin Folk Therapy*, 2020, **28**: 6-8.

[18] Zhang F, Huang J, Liu W, *et al*. Inhibition of drug-metabolizing enzymes by Qingfei Paidu decoction: implication of herb-drug interactions in COVID-19 pharmacotherapy [J]. *Food Chem Toxicol*, 2021, **149**: 111998.

[19] Liu W, Ge GB, Wang Y L, *et al*. Chemical profiling and tissue distribution study of Qingfei Paidu decoction in mice using UHPLC-Q-Orbitrap HRMS [J]. *Chin Tradit Herb Drugs*, 2020, **51**: 2035-2045.

[20] Wu GS, Zhong J, Zheng NN, *et al*. Investigation of modulating effect of Qingfei Paidu Decoction on host metabolism and gut microbiome in rats [J]. *Chin J Chin Mater Med*, 2020, **45**: 3726-3739.

[21] Zhao J, Tian SS, Lu D, *et al*. Systems pharmacological study illustrates the immune regulation, anti-infection, anti-inflammation, and multi-organ protection mechanism of Qing-Fei-Pai-Du decoction in the treatment of COVID-19 [J]. *Phytomedicine*, 2020, **9**: 153315.

[22] Zhao J, Tian SS, Yang J, *et al*. Investigating mechanism of Qing-Fei-Pai-Du-Tang for treatment of COVID-19 by network pharmacology [J]. *Chin Tradit Herb Drugs*, 2020, **51**: 829-835.

[23] Fang SQ, Huang J, Zhang F, *et al*. Pharmacokinetic interaction between a Chinese herbal formula Huosu Yangwei oral liquid and apatinib *in vitro* and *in vivo* [J]. *J Pharm Pharmacol*, 2020, **72**: 979-989.

[24] Zhang F, Huang J, He RJ, *et al*. Herb-drug interaction between Styrax and warfarin: molecular basis and mechanism [J]. *Phytomedicine*, 2020, **77**: 153287.

[25] Chen PY, Yu JW, Lu FL, *et al*. Differentiating parts of Cinnamomum cassia using LC-qTOF-MS in conjunction with principal component analysis [J]. *Biomed Chromatogr*, 2016, **30**: 1449-1457.

[26] Zhang SS, Wu DD, Li H, *et al*. Rapid identification of α-glucosidase inhibitors from *Dioscorea opposita* Thunb peel extract by enzyme functionalized Fe_3O_4 magnetic nanoparticles coupled with HPLC-MS/MSd with HPLC-MS/MS [J]. *Food Funct*, 2017, **8**: 3219-3227.

[27] Ren T, Wang Y, Wang C, *et al*. Isolation and identification of human metabolites from a novel anti-tumor candidate drug 5-chlorogenic acid injection by HPLC-HRMS/MS^n and HPLC-SPE-NMR [J]. *Anal Bioanal Chem*, 2017, **409**: 7035-7048.

[28] Zhang Z, Jiang MY, Wei XY, *et al*. Rapid discovery of chemical constituents and absorbed components in rat serum after oral administration of Fuzi-Lizhong pill based on high-throughput HPLC-Q-TOF/MS analysis [J]. *Chin Med*, 2019, **14**: 6.

[29] Chen LL, Chen CH, Zhang XX, *et al*. Identification of constituents in Gui-Zhi-Jia-Ge-Gen-Tang by LC-IT-MS combined with LC-Q-TOF-MS and elucidation of their metabolic networks in rat plasma after oral administration [J]. *Chin J Nat Med*, 2019, **17**(11): 803-821.

[30] Miyagoshi M, Amagaya S, Ogihara Y. Antitussive effects of L-ephedrine, amygdalin, and Makyokansekito (Chinese traditional medicine) using a cough model induced by sulfur dioxide gas in mice [J]. *Planta Med*, 1986, **52**(4): 275-278.

[31] Wu Z, Kong X, Zhang T, *et al*. Pseudoephedrine/ephedrine shows potent anti-inflammatory activity against TNF-α-mediated acute liver failure induced by lipopolysaccharide/d-galactosamine [J]. *Eur J Pharmacol*, 2014, **724**: 112-121.
[32] Paoletti I, Gregorio V, Baroni A, *et al*. Amygdalin analogues inhibit IFN-γ signalling and reduce the inflammatory response in human epidermal keratinocytes [J]. *Inflammation*, 2013, **36**(6): 1316-1326.
[33] Fiebich B L, Collado J A, Stratz C, *et al*. Pseudoephedrine inhibits T-cell activation by targeting NF-κB, NFAT and AP-1 signaling pathways [J]. *Immunopharm Immunot*, 2011, **34**(1): 98-106.
[34] Deng JG, Li CY, Wang HL, *et al*. Amygdalin mediates relieved atherosclerosis in apolipoprotein E deficient mice through the induction of regulatory T cells [J]. *Biochem Biophys Res Commun*, 2011, **411**(3): 523-529.
[35] Zhang A, Pan W, Lv J, *et al*. Protective effect of amygdalin on LPS-induced acute lung injury by inhibiting NF-κB and NLRP3 signaling pathways [J]. *Inflammation*, 2017, **40**(3): 745-751.
[36] Kant NM, Agrawal AS, Sudeshna B, *et al*. Antiviral activity of baicalin against influenza virus H1N1-pdm09 is due to modulation of NS1-mediated cellular innate immune responses [J]. *J Antimicrob Chemother*, 2014, **69**(5): 1298-1310.
[37] Su HX, Yao S, Zhao WF, *et al*. Anti-SARS-CoV-2 activities in vitro of Shuanghuanglian preparations and bioactive ingredients [J]. *Acta Pharmacol Sin*, 2020, **41**: 1167-1177.
[38] Wu CR, Liu Y, Yang YY, *et al*. Analysis of therapeutic targets for SARS-CoV-2 and discovery of potential drugs by computational methods [J]. *Acta Pharm Sin B*, 2020, **10**(5): 766-788.
[39] Yu JY, Ha JY, Kim KM, *et al*. Anti-inflammatory activities of licorice extract and its active compounds, glycyrrhizic acid, liquiritin and liquiritigenin, in BV2 cells and mice liver [J]. *Molecules*, 2015, **20**(7): 13041-13054.
[40] Zhang Y, Zhang L, Zhang Y, *et al*. The protective role of liquiritin in high fructose-induced myocardial fibrosis *via* inhibiting NF-κB and MAPK signaling pathway [J]. *Biomed Pharmacother*, 2016, **84**: 1337-1349.
[41] Luoliu P D, Li J. Pharmacologic perspective: glycyrrhizin may be an efficacious therapeutic agent for COVID-19 [J]. *Int J Antimicrob Ag*, 2020, **55**(6): 105995.
[42] Bailly C, Gérard Vergoten. Glycyrrhizin: an alternative drug for the treatment of COVID-19 infection and the associated respiratory syndrome? [J]. *Pharmacol Therapeut*, 2020, **214**: 107618.
[43] Murck H. Symptomatic protective action of Glycyrrhizin (Licorice) in COVID-19 infection? [J]. *Front Immunol*, 2020, **11**: 1239.
[44] Huang Y, Zheng SL, Xu ZS, *et al*. Effects of Alismatis rhizome on rat cytochrome P450 enzymes [J]. *Pharmaceut Biol*, 2014, **52**(6): 681-687.
[45] Arnold C, Markovic M, Blossey K, *et al*. Arachidonic acid-metabolizing cytochrome P450 enzymes are targets of {omega}-3 fatty acids [J]. *J Biol Chem*, 2020, **285**: 32720-32733.
[46] Kroetz DL, Zeldin DC. Cytochrome P450 pathways of arachidonic acid metabolism [J]. *Curr Opin Lipidol*, 2020, **13**: 273-283.
[47] Tallima H, Ridi R. Arachidonic acid: physiological roles and potential health benefits-A review [J]. *J Adv Res*, 2017, **11**: 33-41.
[48] Lee W, Ku SK, Bae JS. Antiplatelet, anticoagulant, and profibrinolytic activities of baicalin [J]. *Arch. Pharm. Res.*, 2015, **38**: 893-903.
[49] Kruse JM, Magomedov A, Kurreck A, *et al*. Thromboembolic complications in critically ill COVID-19 patients are associated with impaired fibrinolysis [J]. *Crit Care*, 2020, **24**: 676.
[50] Cremer S, Jakob C, Berkowitsch A, *et al*. Elevated markers of thrombo-inflammatory activation predict outcome in patients with cardiovascular comorbidities and COVID-19 disease: insights from the LEOSS registry [J]. *Clin Res Cardiol*, 2020, **19**: 1-12.
[51] Casale M, Dattilo G, Imbalzano E, *et al*. The thromboembolism in COVID-19: the unsolved problem [J]. *Panminerva Med*, 2020, **16**: 3.

Cite this article as: LIU Wei, HUANG Jian, ZHANG Feng, ZHANG Cong-Cong, LI Rong-Sheng, WANG Yong-Li, WANG Chao-Ran, LIANG Xin-Miao, ZHANG Wei-Dong, YANG Ling, LIU Ping, GE Guang-Bo. Comprehensive profiling and characterization of the absorbed components and metabolites in mice serum and tissues following oral administration of Qing-Fei-Pai-Du decoction by UHPLC-Q-Exactive-Orbitrap HRMS [J]. *Chin J Nat Med*, 2021, **19**(4): 305-320.